ORIGINAL RESEARCH

In Vivo Molecular Characterization of Abdominal Aortic Aneurysms Using Fibrin-Specific Magnetic Resonance Imaging

René M. Botnar, PhD; Julia Brangsch, VMD; Carolin Reimann, VMD; Christian H. P. Janssen, MD; Reza Razavi, MD; Bernd Hamm, MD; Marcus R. Makowski, MD, PhD

***Background*—**The incidence of abdominal aortic aneurysms (AAAs) will significantly increase during the next decade. Novel biomarkers, besides diameter, are needed for a better characterization of aneurysms and the estimation of the risk of rupture. Fibrin is a key protein in the formation of focal hematoma associated with the dissection of the aortic wall and the development of larger thrombi during the progression of AAAs. This study evaluated the potential of a fibrin-specific magnetic resonance (MR) probe for the in vivo characterization of the different stages of AAAs.

***Methods and Results*—**AAAs spontaneously developed in ApoE$^{-/-}$ mice following the infusion of angiotensin-II (Ang-II, 1 μg/kg^{-1}·per minute). An established fibrin-specific molecular MR probe (EP2104R, 10 μmol/kg^{-1}) was administered after 1 to 4 weeks following Ang-II infusion (n=8 per group). All imaging experiments were performed on a clinical 3T Achieva MR system with a microscopy coil (Philips Healthcare, Netherlands). The development of AAA-associated fibrin-rich hematoma and thrombi was assessed. The high signal generated by the fibrin probe enabled high-resolution MR imaging for an accurate assessment and quantification of the relative fibrin composition of focal hematoma and thrombi. Contrast-to-noise-ratios (CNRs) and R1-relaxation rates following the administration of the fibrin probe were in good agreement with ex vivo immunohistomorphometry (R^2=0.83 and 0.85) and gadolinium concentrations determined by inductively coupled plasma mass spectroscopy (R^2=0.78 and 0.72).

***Conclusions*—**The fibrin-specific molecular MR probe allowed the delineation and quantification of changes in fibrin content in early and advanced AAAs. Fibrin MRI could provide a novel in vivo biomarker to improve the risk stratification of patients with aortic aneurysms. **(*J Am Heart Assoc*.2018;7:e007909. DOI: 10.1161/JAHA.117.007909)**

Key Words: abdominal aortic aneurysm • fibrin • imaging • magnetic resonance imaging

Diseases of the cardiovascular system still represent the main cause of death in Western societies. In this group, specifically, diseases of the aorta demonstrate an increase in incidence.[1,2] In the group of cardiovascular diseases, the rupture of aortic aneurysms currently represents the third most common cause of sudden death, with myocardial infarction and stroke representing numbers one and two. In the general population older than 50 years, the incidence of abdominal aortic aneurysms (AAAs) is ≈5%. Currently, more than 70 000 interventions and operations are performed for the treatment of AAAs in the United States.[3,4] Even though AAAs represent a relevant disease, the exact pathophysiological mechanisms leading to their development are still unknown. Therefore, a large number of aneurysms are classified to have a nonspecific cause.[5] For only a limited number of aneurysms, definite causes are known and can be defined. These include infections, connective tissue disorders (eg, Marfan disease) and trauma. Independent of the cause, it is thought that the rupture of the elastic laminae in the tunica media leads to the dissection of the aortic wall. This subsequently leads to a progressive dilation of the aortic lumen. If these processes remain unrecognized and untreated, an aortic rupture with fatal implications for the patient can be the consequence.[6]

For the tensile strength of the aortic wall, the extracellular matrix plays the most important role. The highest expressed proteins in the tunica media are collagen and elastic fibers. They contribute most to the tensile strength to withstand the

From the Division of Imaging Sciences (R.M.B., C.H.P.J., R.R., M.R.M.), BHF Centre of Excellence (R.M.B., R.R.), Wellcome Trust and EPSRC Medical Engineering Center (R.M.B., R.R.), and NIHR Biomedical Research Centre (R.M.B., R.R.), King's College London, London, United Kingdom; Department of Radiology, Charite, Berlin, Germany (J.B., C.R., B.H., M.R.M.).

Accompanying Data S1 and Figures S1, S2 are available at http://jaha.ahajournals.org/content/7/11/e007909/DC1/embed/inline-supplementary-material-1.pdf

Correspondence to: Marcus R. Makowski, MD, PhD, Department of Radiology, Charité, Berlin, Germany.
Division of Imaging Sciences, King's College London, London, United Kingdom.
E-mails: marcus.makowski@charite.de; marcus.makowski@kcl.ac.uk

Received October 19, 2017; accepted January 24, 2018.

Clinical Perspective

What Is New?

- The fibrin-specific probe used in this study enables the differentiation between acute and old abdominal aortic aneurysms (AAA)-associated thrombi in a mouse model.
- Acute AAA-associated thrombi show a high-contrast enhancement associated with a high content of fibrin.
- Older AAA-associated thrombi show a low-contrast enhancement associated with a low content of fibrin.

What Are the Clinical Implications?

- Fibrin magnetic resonance imaging could provide a novel in vivo biomarker to improve the risk stratification of patients with aortic aneurysms.
- The fibrin-specific probe allowed an in vivo differentiation between newly formed fibrin-rich thrombi and advanced remodeled thrombi.
- Such a parameter could be valuable for an improved characterization of AAA-associated thrombi in vivo.
- This is especially relevant in the context of clinical studies demonstrating that the D-dimer correlates with AAA growth.

arterial pulsation and high intravascular pressure.[7] Most postmortem histopathologic studies agree that the breakdown of collagen and elastic fibers in the aortic wall leads to a weakening and progressive dilation of the aorta, resulting in the development of an aneurysm.[8] Specifically, the rupture of elastic laminae in the tunica media leads to an aortic dissection. This results in the activation of the blood-clotting cascade, the accumulation of fibrin at the rupture site with the development of a focal fibrin-rich hematoma in the aortic wall.[9] If the aneurysm continues to increase in size, a large fibrin-rich thrombus is formed. Following that, the aneurysmal tissue matures and the fibrin-rich matrix is increasingly replaced and stabilized by other extracellular matrix proteins, including collagen and elastin.[9–11] It is thought that the balance between the synthesis and degradation of these extracellular matrix proteins in the ruptured aortic wall and thrombus determines the further progression and outcome of AAAs.[9] In this context, the D-dimer has been recently proposed as the most promising novel biomarker for an improved characterization of aortic aneurysms in a clinical setting.[12–14] The D-dimer represents a fibrin fragment, which is formed during the blood-clotting cascade following aortic dissection. Its concentration correlates with the development of a focal hematoma and thrombus size. This underlines the important role that fibrin plays during the initiation and progression of aortic aneurysms.[12–14]

In clinical practice, AAAs are currently diagnosed by computed tomography angiography, magnetic resonance (MR) angiography, or ultrasound. Besides the diameter, there is currently no clinically established biomarker available to improve the characterization of aneurysms and predict the risk of rupture.[6,15]

In this study, we hypothesize that a fibrin-specific molecular MR probe allows for the detection of an early focal mural hematoma associated with an aortic dissection, before the dilation of the aorta. Additionally, early and late AAA-associated thrombi can be differentiated based on their relative fibrin composition.

Methods

The data, analytic methods, and study materials will not be made available to other researchers for purposes of reproducing the results or replicating the procedure.

Animal Experiments

Homozygous C57BL/6J ApoE-knockout mice (male) were acquired from Charles Rivers Laboratories (Edinburgh, UK). Housing and care of animals and all the procedures performed in this study were in accordance with the guidelines and regulations of the United Kingdom Home Office. Eight-week-old mice were implanted with minipumps (Alzet model 2004, Durect Corp). Angiotensin II was administered continuously by subcutaneous infusion at a dose of 1 $\mu g/kg^{-1}$ per minute.[9,16] magnetic resonance imaging (MRI) was performed at weeks 1, 2, 3, and 4 after the start of AngII infusion (n=8 per group, Figure S1). Tissue was harvested for further processing each week (n=8 per group, Figure S1). Sham-operated mice served as the control group. These animals were also implanted with minipumps but instead of angiotensin II, saline was infused for 4 weeks (sham-operated group, n=6). At each time point, 8 animals were scanned by MRI before and following the administration of the control probe (gadopentetate dimeglumine, Bayer Healthcare AG, Berlin) and additionally before and following the administration of the fibrin-specific molecular probe. Within 48 hours, 2 imaging sessions were performed. The first imaging session included imaging before and following the administration of 0.2 $mmol/kg^{-1}$ gadopentetate dimeglumine (Gd-DTPA) to study the unspecific uptake in the aortic wall. The second imaging session included imaging before and following the administration of 10 $\mu mol/kg^{-1}$ of an established fibrin-specific molecular probe.[17–20] Following the two imaging sessions, mice were euthanized for histopathology, immunohistopathology, and inductively coupled plasma mass spectroscopy (ICP-MS). Additionally, competition experiments were performed (please see Data S1).

For each imaging session, animals were anesthetized by intramuscular injection of a combination of medetomidine (500 $\mu g/kg^{-1}$), fentanyl (50 $\mu g/kg^{-1}$), and midazolam (5 mg/kg^{-1}). Following the imaging session, a combination of

antidotes was administered to shorten anesthesia time. A combination of atipamezole (2.5 mg/kg^{-1}), naloxone (1200 μg/kg^{-1}), flumazenil (500 μg/kg^{-1}) was used.[21] These techniques have been previously described in detail.[22,23] Following the last imaging session, terminal exsanguination by anterior perfusion with phosphate buffered saline with a pressure of 100 mm Hg. If vessel samples were used for histology, this was followed by a perfusion with 10% formalin. To allow for anatomic matching, the aorta was excised including the right renal artery and last pair of intercostal arteries.

In Vivo Molecular MR Imaging

Following the administration of the anesthesia, all animals were positioned on a surface microscopy coil (4.7 cm, Philips Healthcare, Best, Netherlands). For all imaging experiments, a clinical 3T Achieva MR system was used (Philips Healthcare, Best, Netherlands). The system was equipped with a clinical gradient system (30 mT/m^{-1}, 200 mT/m^{-1}·per millisecond). Additionally, a dedicated software package for cardiac imaging was available. For imaging, all animals were in a supine position. Signal was received using a microscopy single loop coil. To maintain the body temperature (37°C) of animals during the imaging sessions, a dedicated MR-compatible heating system was used (Model 1025, SA Instruments Inc, Stony Brook, NY).

The imaging protocol included the following sequences. First, a low-resolution scout scan (3-dimensional gradient echo sequence) was used for an anatomic overview and to localize the abdominal aorta. In the next step, a 2-dimensional time-of-flight (2D TOF) angiography was performed in the transverse orientation for a specific visualization of the abdominal aorta. Imaging parameters included: imaging matrix=160×160, field of view=20×20×10 mm, slice thickness=0.5 mm, inplane spatial resolution=0.3×0.3 mm (reconstructed 0.13×0.13 mm), flip angle=60°, repetition time (TR) sequence=37 ms and echo time (TE) 7.7 ms. Based on the TOF angiography, a maximum intensity projection (MIP) was automatically reconstructed. Based on this MIP, with the visualization of the intra-abdominal arteries, the following scans (T1 delayed-enhancement MRI, T1 mapping) could be exactly planned in the region of interest on the abdominal aorta. Prior to the T1 delayed-enhancement scan, a I\Look-Locker sequence (2-dimensional) was planned on the aorta to determine the nulling time (inversion time, TI) for blood. This approach is comparable to the late enhancement imaging approach in the myocardium. Imaging parameters for the Look-Locker were: matrix=75×75, field of view=30 mm, slice thickness=2 mm, inplane resolution=0.4×0.4, TR=19 ms, TE=8.6 ms, and flip angle=10°. The repetition time between inversion recovery (IR) pulses was constant with 1 second. The following imaging parameters were used for the inversion recovery delayed-enhancement MRI scans (3D IR fast gradient echo scans) for the visualization and quantification of the molecular probes. matrix=30×30 mm, field of view=30 mm, slice thickness=0.5 mm, reconstructed slice thickness=0.25 mm; 40 slices were acquired, inplane spatial resolution=0.1 mm, TR=28 ms, TE=8.2 ms, and flip angle=30°. The repetition time between IR pulses was constant with 1 second. Please see Data S1 for additional information regarding T1 mapping techniques and the in vivo competition experiments.

MR Image Analysis

Analysis of all resulting DICOM (Digital Imaging and Communications in Medicine) images was performed using OsiriX (version 7.1, OsiriX foundation). To localize the aortic wall and aortic aneurysms, the high-resolution late-enhancement images were automatically coregistered with the TOF images based on the location data in the DICOM headers. All morphometric measurements were performed on the high-resolution late-enhancement images before and following the administration of the control agent (gadopentetate dimeglumine) and the fibrin-specific molecular probe. For the assessment of signal intensities, regions of interest were measured as areas of signal enhancement on high-resolution late-enhancement images in relation to the TOF images. For these regions, the contrast-to-noise ratio (CNR) was calculated using the following formula: CNR=(combined vessel wall and aneurysmal aortic tissue signal−blood signal)/noise. The signal of noise was determined as the standard deviation measured in the air anterior to the aneurysmal aortas.

Inductively Coupled Mass Spectroscopy

To measure the local concentration of the molecular probe, ICP-MS was performed in a subgroup of aneurysmal aortic tissue samples (n=3 per group).

For a reproducible analysis of the local gadolinium concentration, tissue samples were digested overnight at 37°C using 70% nitric acid. For the ICP-MS analysis, tissue samples were diluted with deionized water. For each analysis, a standard curve was acquired for the concentration of gadolinium.

Histologic and Immunohistochemical Analysis of Aortic Aneurysms

Following the surgical removal of aortic aneurysms, tissues were processed overnight for further histologic analysis. For sectioning, aortic aneurysms were embedded in paraffin.

Histologic sections (6 μm) were cut every 40 μm along the aortic aneurysm. Sectioning was started from the proximal end of the aneurysm. Sections were stained for Miller's Elastica van Gieson stain (EvG), Masson Trichrome (collagen), and hematoxylin and eosin.

Immunohistochemical staining for fibrin was performed using a fibrin-specific antibody (mouse anti-fibrin-antibody, 1/200 diluted, American Diagnostica, Stamford, CT, USA). Prior to staining, sections were blocked for 10 minutes with DAKO block at room temperature. Following incubation with the primary antibody for 60 minutes, slides were washed with Dulbecco's phosphate-buffered saline at pH of 7.4 at room temperature. In the next step, sections were stained for 60 minutes with a polyclonal rabbit anti-mouse IgG:Biotin (DAKO, diluted 1/150) antibody. For signal generation extravidin peroxidase (diluted 1/100) was used. The peroxidase activity was measured using the Vector SG substrate kit (Vector Laboratories, Peterborough, UK). For each histologic slide 100 μL of chromagen substrate was added for 15 minutes. Histologic slides were then washed with Dulbecco's phosphate-buffered saline, pH 7.4 (5 min/wash) 3 times, which was followed by a rinse for 5 minutes in running tap water. Nuclear Fast Red (Vector Laboratories) was used to counterstained tissue sections for 10 to 15 minutes. These techniques have been described previously.[24]

Statistical Analysis

Values are expressed as mean±standard deviation. A Student *t* test (two-tailed, unpaired) was used to compare continuous variables. In case of more than 2 groups, statistical comparisons were performed by analysis of variance (ANOVA) followed by the Bonferroni correction. A *P* value of 0.05 was considered statistically significant.

Results

Development of Aortic Aneurysms on MR Angiography

In the control group (sham group, apoE$^{-/-}$ mice) after 4 weeks of saline infusion using osmotic mini pumps, no aortic dilation or development of aneurysms was observed (n=6, Figures 1A, 2A, 2andB). In the aneurysm group, the continuous infusion of 1 μg/kg^{-1}·per minute angiotensin II via osmotic minipumps resulted in the formation of suprarenal aortic aneurysms (Figures 2 and 3). Different previous studies have described this to be the prevalent site of aneurysm formation in this mouse model.[9,16,25] Following the initiation of the angiotensin II infusion, animals were imaged after 1 to 4 weeks (n=8 per group). After 2 weeks of angiotensin II infusion, a significant increase (P<0.05) in abdominal aortic areas was observed on the time of flight angiography as well as on ex vivo histological measurements (Figure 1A). The aortic areas continued to increase during weeks 3 and 4 (P<0.05; Figure 1A). In vivo cross-sectional area measurements based on the TOF angiography correlated strongly (R^2=0.83, y=0.96x+0.38) with the ex vivo area measurements (Figure 1B). Area measurements on the TOF angiography slightly overestimated the size of aortic aneurysms compared with histology. Arterial rupture led to death through loss of blood into the abdominal cavity before imaging in 3 mice. These mice were excluded from the study and replaced.

Molecular Imaging of Thrombus Detection Using the Fibrin-Specific Molecular Probe

Animals were imaged before and following the administration of the nonspecific control agent (gadopentetate dimeglumine) and the fibrin-specific molecular probe. In both groups of mice

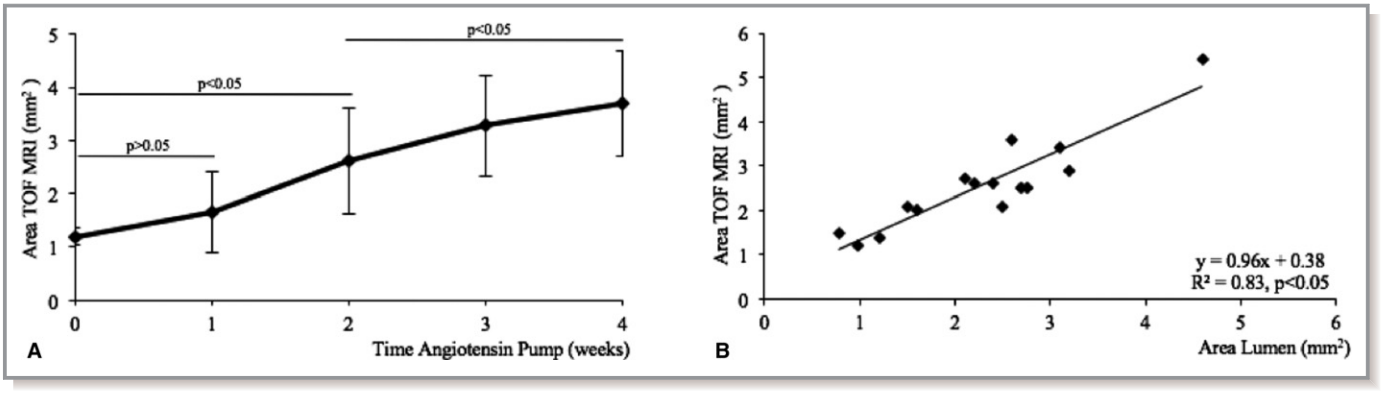

Figure 1. Development of aortic aneurysms in the ApoE$^{-/-}$ mouse model. A, On in vivo MRI images, a gradual increase in aortic cross-sectional areas was measured over the 4-week time course of angiotensin II infusion in the ApoE$^{-/-}$ mouse model. A significant (P<0.05) increase was measured after 2 to 4 weeks compared with the control (sham) group. B, In vivo cross-sectional area measurements on the TOF angiography significantly correlated (P<0.05) with ex vivo area measurements on histology (EvG stain). Values are expressed as means±SD. MRI indicates magnetic resonance imaging; TOF, time of flight.

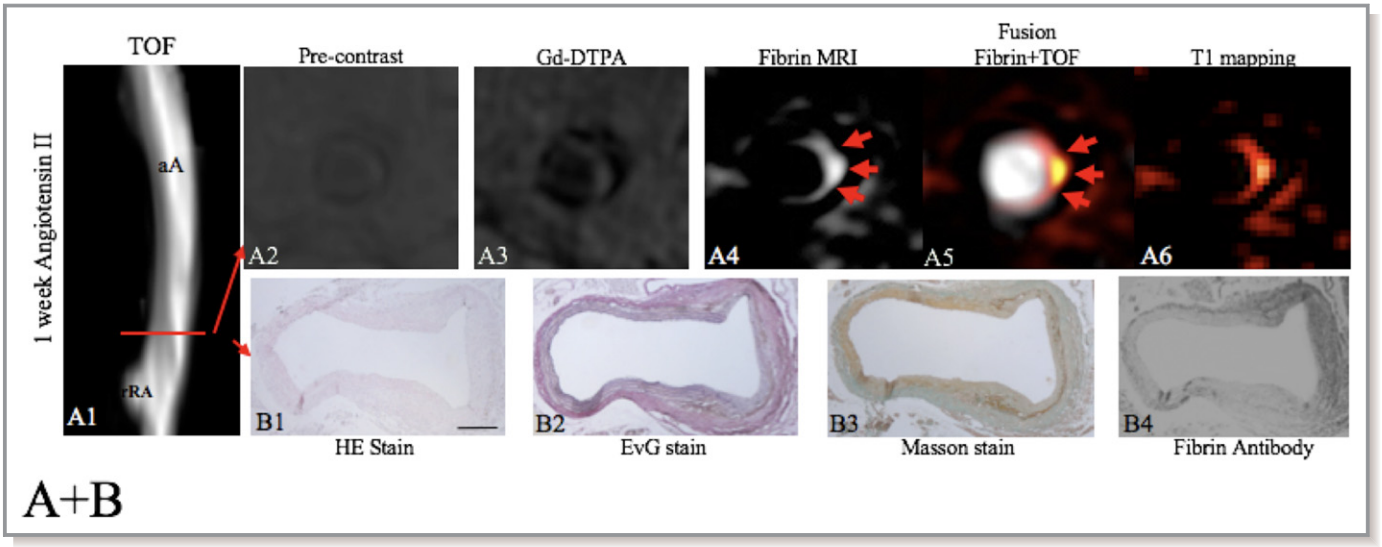

Figure 2. Assessment of a focal fibrin-rich intramural hematoma before the dilation of the aorta by fibrin MRI. A, On the TOF angiogram, a nondilated aortic lumen without luminal irregularities can be appreciated in an ApoE$^{-/-}$ mouse 1 week after continuous infusion of angiotensin II. The red line indicates the alignment of in vivo MRI sequences and ex vivo histology. No significant enhancement of the aorta was measured on precontrast scans (A2) and following the administration of the nonspecific control agent (Gd-DTPA, A3). Following the administration of the fibrin-specific molecular probe, a strong focal enhancement was measured at the dissection side (A4–A6). On the EvG stain, the dissection of elastic laminae can be clearly visualized on magnified images (B2). In between the dissection, a fibrin-rich mural hematoma can be visualized (B2–B4). It's a strong signal from the fibrin that antibody was measured at the location of the intramural hematoma (B4). No relevant formation of elastin or collagen fibers was measured in the hematoma on histologic sections (B1–B3), indicating that no remodeling of the hematoma has occurred. aA indicates abdominal aorta; Gd-DTPA, gadopentetate dimeglumine; MRI, magnetic resonance imaging; rRA, right renal artery; TOF, time of flight.

(sham and Ang-II infusion), there was no significant (P>0.05) signal enhancement (Figures 2 and 3) of the aortic or aneurysmal wall in both native MRI and after administration of the nonspecific control agent (Gd-DTPA). In the sham-treated mice there was also no significant (P>0.05) signal enhancement after the administration of the fibrin-specific probe.

In vivo visualization of the aortic dissection site before aortic dilation

In the aneurysm group, the continuous angiotensin II infusion resulted in the dissection of the aortic wall with the rupture of the elastic laminae in the tunica media. This was observed in all stages of AAA development (Figure 2B2). The dissection of the aortic wall was associated with the development of a small intramural hematoma at the location where the elastic laminae ruptured (Figure 2B3 and B4). Additionally, the formation of a large extramural hematoma could be observed, especially in advanced aortic aneurysms after 3 and 4 weeks (Figure 3). At the early stage of aneurysm development, after 1 week of angiotensin II infusion, a strong focal signal could be measured in the aortic wall following the administration of the fibrin-specific molecular probe. At this stage, no relevant dilation of the aorta could be measured in vivo on the MR angiogram. Corresponding histologic analysis confirmed the presence of an aortic dissection with the rupture of elastic laminae and the formation of a small focal hematoma (Figure 3B2–B4). Ex vivo staining for fibrin confirmed the formation of a fibrin-rich thrombus at that location (Figure 3B4). Corresponding to histopathology, the fibrin-specific molecular probe allowed the detection of the rupture site before the dilation of the aorta (Figure 3A4–A6). In these small focal hematoma, no relevant expression of elastin or collagen was measured on histologic sections (Figure 3B2, B3). This indicates that no tissue remodeling in the matrix of the hematoma has occurred yet.

In vivo characterization of thrombi associated with the formation of an aortic aneurysm

Following the infusion of angiotensin II, thrombi associated with the development of aortic aneurysms were observed (Figure 3A and 3B). In the early phases after 2 to 3 weeks, these relatively large thrombi showed high CNRs following the administration of the fibrin-specific molecular probe (Figure 3A4–A6). This high signal correlated with a strong staining for fibrin on ex vivo immunohistopathology in these thrombi (Figure 3B4). In the later phases of thrombus development after 4 weeks, a significant reduction in CNRs was observed within the matrix of the thrombi following the administration of the fibrin-specific probe (Figure 3C4–C6). Thrombi were still detectable; however, the signal from the fibrin-specific molecular probe was significantly reduced. In vivo signal measurements correlated with an overall

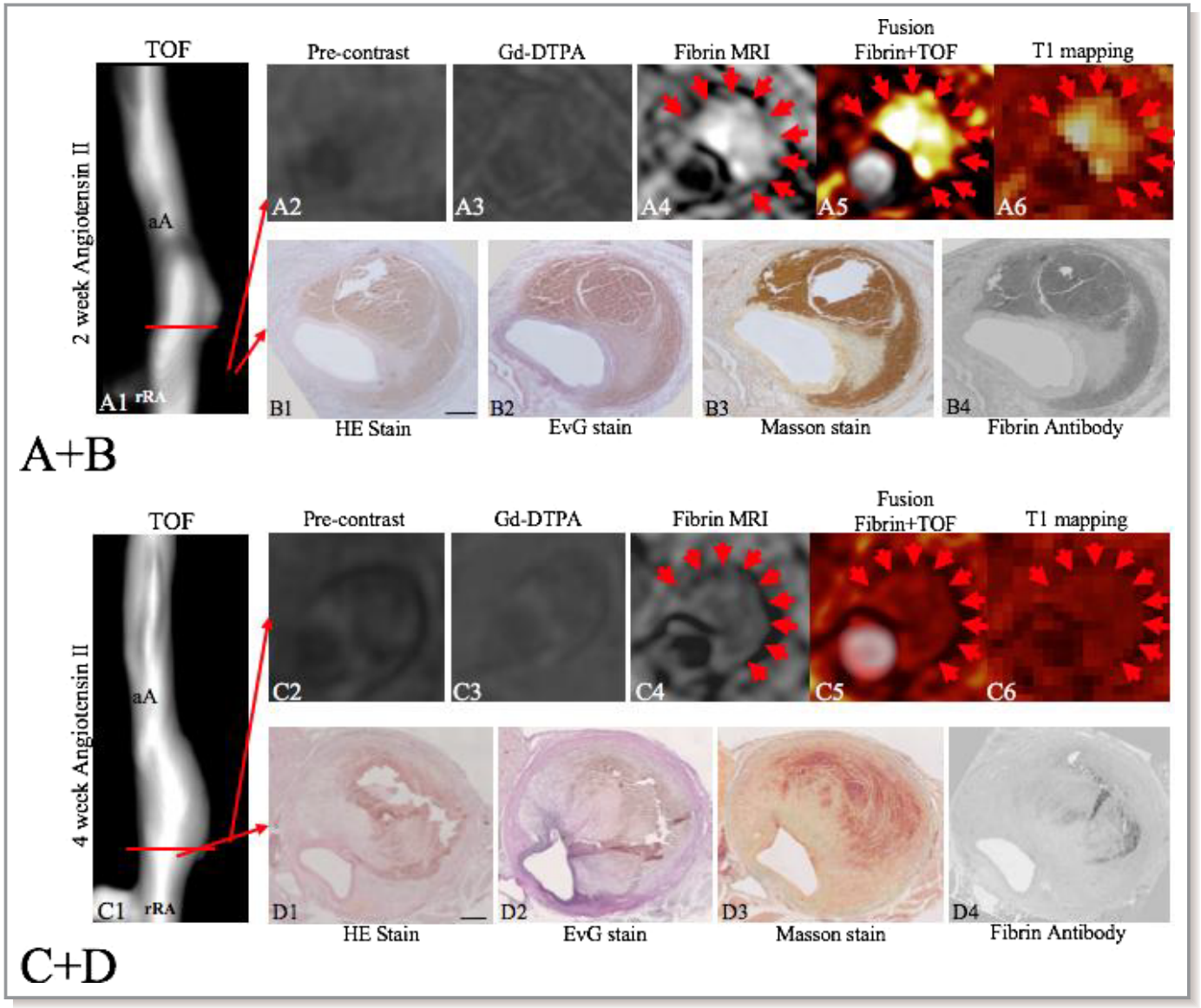

Figure 3. Visualization of early and advanced/remodeled AAA-associated thrombi by fibrin MRI. A and B, After 2 weeks of angiotensin II infusion, the formation of a suprarenal aortic aneurysm was observed on the TOF angiogram (A1). On precontrast scans and control scans with Gd-DTPA, no significant enhancement was measured. On the fibrin MRI scan, a strong signal enhancement was measured at the location of the fibrin-rich thrombus (A4–A6, red arrows). Corresponding histology and immunohistochemistry show the formation of a fresh fibrin-rich thrombus with a strong signal using the fibrin-specific antibody. In areas adjacent to the thrombus, only a few elastin and collagen fibers were observed (B1–B4), indicating that no remodeling took place yet. C and D, After 4 weeks of angiotensin II infusion, the formation of advanced suprarenal aortic aneurysm was observed on the TOF-angiogram (C1). On precontrast scans and control scans with Gd-DTPA, no significant enhancement was measured. On the fibrin MRI scan, a weak-to-moderate signal enhancement was measured at the location of the fibrin-rich thrombus (C4–C6, red arrows). Corresponding histology and immunohistochemistry shows the formation of an advanced/remodeled thrombus with a weak signal using the fibrin-specific antibody. In areas adjacent to the thrombus, significant expression of elastin and collagen fibers was measured (D2–D4,), indicating that remodeling took place. Compared with earlier stages of AAA formation (A+B), a strong increase in expression of elastin and collagen fibers was measured directly adjacent to the thrombus. aA indicates abdominal aorta; Gd-DTPA, gadopentetate dimeglumine; MRI, magnetic resonance imaging; rRA, right renal artery; TOF, time of flight.

decreased expression of fibrin within the thrombus on ex vivo immunohistopathology. On the other hand, an increased remodeling of the thrombus was observed with a significantly increased expression of collagen and elastic fibers within the matrix of the thrombus in all animals 3 to 4 weeks after continuous Ang-II infusion (Figure 4B). Based on these measurements, the fibrin-specific molecular probe enabled the differentiation between early thrombi formation and late-stage remodel thrombi. As already suggested in previous studies,[9] the balance of extracellular matrix degradation and formation in AAA-associated thrombi is an important factor in the progression and outcome of aortic aneurysms.

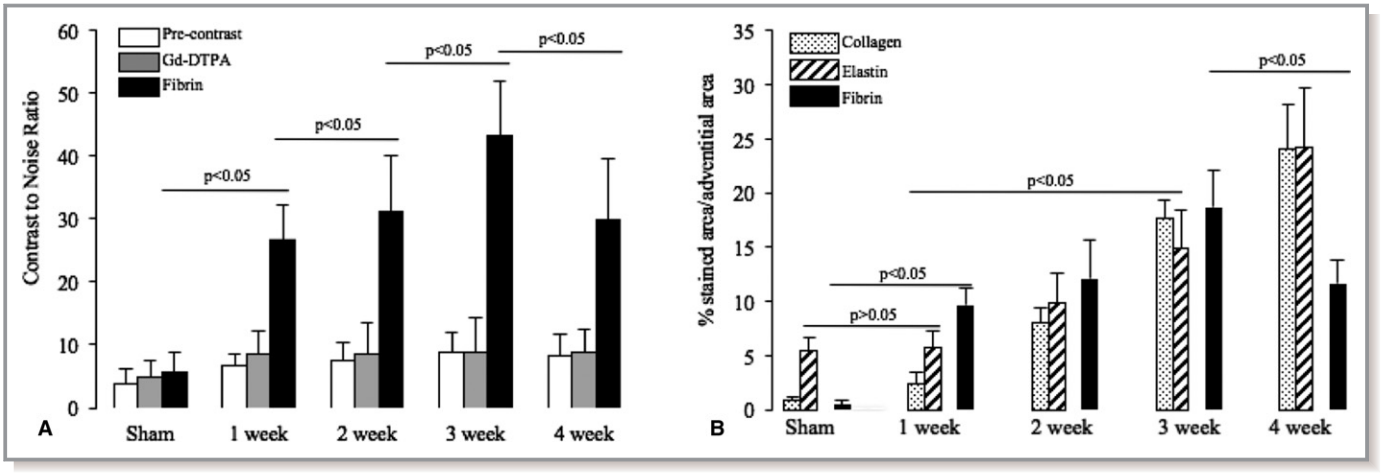

Figure 4. In vivo assessment of fibrin expression and time course of remodeling of AAA-associated thrombi regarding fibrin, elastin, and collagen fibers. A, Comparison of average CNR values calculated from measurement on precontrast scans, control scans for Gd-DTPA, and fibrin MRI (n=8 per aneurysm group, n=6 sham group). A significant and steady increase in CNR could be observed with increasing time of angiotensin II infusion in weeks 1 to 3. In week 4, a significant decrease on fibrin MRI was measured compared with week 3, indicating the increased remodeling of thrombi with a replacement of fibrin. B, Graph demonstrating the time course of remodeling of AAA-associated thrombi from 1 to 4 weeks following angiotensin II infusion. In the control group (sham), no relevant expression of collagen or fibrin was observed, only the normal elastin expression in the elastic laminae of the aortic wall. After 1 week of angiotensin II infusion, a strong expression of fibrin was observed in thrombi, and no relevant expression of collagen or elastin was measured, compared to the sham group. The expression of collagen and elastin gradually increased in weeks 2, 3, and 4, indicating the progressive remodeling of the thrombus. Fibrin expression also increased in weeks 2 and 3. Fibrin was, however, increasingly replaced by collagen and elastin in week 4. AAA indicates abdominal aortic aneurysm; CNR, contrast-to-noise ratio; Gd-DTPA, gadopentetate dimeglumine; MRI, magnetic resonance imaging.

CNR and T1 Mapping

On vessel wall scans before the administration of the fibrin-specific molecular probe (precontrast) and after administration of Gd-DTPA, a relatively low CNR and R1 on T1 relaxation maps in the aortic wall in all mice (sham and Ang-II infusion) was measured (Figure 4A). Following the administration of the fibrin-specific molecular probe, a strong and significant ($P<0.05$) increase in CNR and R1 was measured at the aortic dissection site before aortic dilation starting from 1 week of Ang-II infusion. These in vivo measurements of CNR and R1 were in close and significant ($P<0.05$) agreement with the ex vivo quantification of fibrin density on immunohistochemistry sections. A minor, however not significant ($P>0.05$), progressive increase in CNR and R1 could also be observed on precontrast and Gd-DTPA scans. This effect was due to the minor intrinsic T1 shortening effect of intramural thrombi. No significant difference ($P>0.05$) in vessel wall enhancement (CNR, R1) was detected between precontrast scans on day 2 and precontrast scans on day 1 (n=3 per group). Signal effects from potentially remaining control agent (Gd-DTPA) in the vascular wall could therefore be excluded.

Competition Experiments

The signal enhancement of precontrast scans in imaging session 1 (CNR 3.9±0.6, Figure S2) did not differ ($P>0.05$) from the signal enhancement of the other investigated animals at the same time point in this study (4 weeks of angiotensin II infusion). The administration of the gadolinium-labeled fibrin-specific molecular MR probe (EP2104R, 10 $\mu mol/kg^{-1}$) resulted in a marked increase of CNR (29.4±6.6, $P\leq0.05$), compared with the precontrast scan. Forty-eight hours later at imaging session 2, initially a precontrast scan was performed. The precontrast scan yielded a CNR of 4.1±1.3, which was not significantly ($P>0.05$) different from the precontrast scan during imaging session 1. In the next step, the injection of 100 $\mu mol/kg^{-1}$ of the unlabeled imaging probe peptide did not results in a significant ($P>0.05$) increase of CNR (4.2±1.7). In the final step, the Gd-labeled fibrin-specific molecular MR probe (EP2104R, 10 $\mu mol/kg^{-1}$) was administered. This resulted in a significantly decreased ($P\leq0.05$) CNR compared with the probe injection during session 1. No significant difference ($P>0.05$) was found between the precontrast scan during session 1 and session 2.

Gadolinium Concentration by Inductively Coupled Mass Spectroscopy

The average concentration of gadolinium in the aneurysmal aortic wall increased substantially as disease progressed from the initial to advanced stages after 2 and 3 weeks. A significant decrease ($P<0.05$) in the gadolinium concentration was observed after 4 weeks, compared with the 3-week group. A significant correlation of CNR (y=1.2x−0.88,

R^2=0.78, P<0.05) and R1 (y=0.31x−0.75, R^2=0.72, P<0.05) with ex vivo measured gadolinium concentrations (ICP-MS) was found.

Discussion

In this molecular MR imaging study, we report the in vivo characterization of aortic aneurysms using a fibrin-specific molecular probe. The fibrin-specific probe enabled the noninvasive detection of the aortic dissection site before aortic dilation by the visualization of the small fibrin-rich hematoma at the dissection site. In advanced aortic aneurysms, the probe enabled the characterization of the relative fibrin expression within the matrix of AAA-associated thrombi. In early thrombi, a strong in vivo signal and a high relative fibrin composition could be measured, which was confirmed by ex vivo analysis. In advanced thrombi, an increased remodeling of the matrix of the thrombus occurred and a relative decrease in fibrin expression was measured in vivo. These changes could be visualized and quantified in vivo by the fibrin specific probe and ex vivo by immunohistopathology. Relative changes in fibrin composition of the thrombus at different remodeling stages could therefore be monitored noninvasively.

The signal enhancement measured by the fibrin-specific molecular probe differed markedly from the measurements resulting from the commonly used control contrast agent, Gd-DTPA, for which no significant accumulation was measured. In vivo aneurysmal CNR and R1 values following the administration of the fibrin-specific probe were in good agreement with ex vivo gadolinium concentrations as determined by ICP-MS.

There are various potential applications for a fibrin-specific probe in the context of AAAs. Unlike existing clinical approaches, which are based on aneurysmal cross-sectional area or diameter measurements for risk evaluation, fibrin-specific MRI enables the assessment of alterations within the arterial wall at the molecular level.

In Vivo Visualization of Focal Hematoma Associated With the Aortic Dissection Site Before Aortic Dilation

Even though human AAAs represent a relatively frequent vascular disease, their pathogenesis is not fully understood yet. This is attributable to the difficulty in obtaining in vivo tissue samples from aortic aneurysms. In contrast, it is relatively easy to obtain tissue samples from atherosclerotic plaques, eg, during carotid endarterectomy; therefore, substantially more data exist for the molecular characterization of atherosclerosis. Previous studies investigating the development of AAAs mainly relied on postmortem tissue samples from patients who died of aortic aneurysm rupture. Typical pathologic features of these late-stage or ruptured aneurysms include adventitial hypertrophy, the accumulation of proinflammatory cells and the high expression of extracellular matrix proteins, such as collagen and elastic fibers.[26,27] Limited in vivo and ex vivo data are currently available regarding the pathophysiologic processes in AAAs and the composition of early-stage human AAAs. Different studies have, however, indicated that aortic dissection, which includes the rupture of elastic laminae, could be one of the initiating events for the onset and progression of human AAAs.[9,28]

In this experimental study, the initiating event for the development of AAAs was the dissection or rupture of the elastic laminae in the tunica media of the aorta. Subsequently, a focal mural fibrin-rich hematoma developed. This fibrin-rich hematoma could be clearly visualized using the fibrin-specific molecular probe. Other groups have also observed the formation of a focal hematoma in this model.[9] This is the first study to demonstrate that a fibrin-specific probe allows noninvasive detection of the aortic dissection sites on a molecular level before a dilation of the aortic can be observed. This observation is in line with measurements of the D-dimer in patients. The D-dimer has even been proposed as a parameter to rule out or confirm an aortic dissection.[29]

Characterization of AAA Associated Thrombi

In patients with aortic aneurysms, an associated thrombus usually develops. Following the development of mural thrombi, the degree of remodeling of the matrix of the thrombi is thought to be an important factor for a potential further progression and rupture of aortic aneurysms.[9] Different studies have also shown that compensatory repair mechanisms, which include the remodeling of the thrombus, lead to a stabilization of the aneurysm and, in some cases, to a reduction of size.[30] These studies support the assumption that compensatory remodeling mechanisms, which lead to a relative decrease in fibrin and relative increase in other extracellular matrix proteins such as collagen and elastic fibers, play an important role in stabilizing the aneurysm and the thrombus in patients with AAAs.[11] Previous molecular imaging studies have already investigated the potential of thrombus imaging.[31]

In our study, a fibrin-specific molecular probe enabled the visualization and characterization of AAA-associated thrombi in vivo. In the early phases of thrombus development, thrombi are rich in fibrin, which results from the cross-linking of fibrinogen to the fibrin mesh. These fresh fibrin-rich thrombi could be detected with a high signal using the fibrin-specific molecular probe. In later stages with advanced remodeling of the thrombus, the relative amount of fibrin decreases, while the relative amount of other extracellular matrix proteins,

including collagen and elastin increases. This type of thrombi could be detected with a significantly reduced signal from the fibrin-specific probe.

The fibrin-specific probe therefore allowed an in vivo differentiation between newly formed fibrin-rich thrombi and advanced remodeled thrombi. Such a parameter could be valuable for improved characterization of AAA-associated thrombi in vivo. This is especially relevant in the context of clinical studies demonstrating that the D-dimer correlates with AAA growth.[12] These results are in line with previous studies, that have also reported a decrease in fibrin probe binding to older thrombi.[32,33]

Clinical Screening for and Characterization of Aortic Aneurysms

In patients with suspected aortic aneurysms, computed tomography angiography, magnetic resonance angiography, and ultrasonography are the most frequently used imaging techniques for the initial assessment and follow-up of patients.[34] It is currently recommended that small asymptomatic AAAs (smaller than 3.5 cm) are closely monitored by imaging. For larger AAAs (larger than 5.5 cm), endovascular repair or aortic surgery is recommended.[6] However, there is still discussion regarding the optimal management of medium-sized AAAs (4–5.5 cm).[6,15] This controversy reflects that novel biomarkers are needed for an improved assessment of aortic aneurysms. Currently, the only clinically established marker is represented by the in vivo measurement of the aortic diameter. Different studies have shown that this parameter has limitations regarding the prognosis of progression and rupture.[6,15]

Regarding novel biomarkers for the assessment of AAAs, the D-dimer has shown great promise. The D-dimer represents a fibrin fragment that is formed following endothelial damage and the activation of repair processes. Different studies showed a correlation between AAA diameter growth and D-dimer values. The higher the plasma concentration of the D-dimer, the faster the observed growth rate of the aneurysm was.[12] Additionally, a meta-analysis showed that D-dimer concentration and aneurysm diameter have a strong linear positive association.[13] It was even suggested that a relative cutoff value of D-dimer could be used to define the imaging follow-up interval of aortic aneurysms.[12] These observations regarding the D-dimer were supported by a recent postmortem study demonstrating that the majority of AAAs are associated with nonocclusive murine thrombi and that fibrin plays an important role during the early thrombus formation and advanced thrombus remodeling.[14]

In this context, a fibrin-specific molecular probe could be useful for further in vivo characterization of AAA-associated thrombi remodeling. Thereby, it could provide information for a more accurate risk stratification of patients with AAAs. Additionally, such a probe could be useful for the detection of minor AAA-associated fresh hematomas in the aortic wall as well as for the differentiation of early and old AAAs.

In the current clinical setting, molecular gadolinium-based MR probes are not available. However, in the context of atherosclerosis imaging, unspecific probes have shown potential for an improved characterization of the composition of the arterial wall.[35]

Translation of the Fibrin-Specific Molecular Probe Into a Clinical Setting

MRI allows imaging of molecular probes with high spatial resolution; it is, however, associated with a lower sensitivity for probe detection compared with, eg, nuclear medicine techniques such as positron emission tomography. To overcome this limitation, a probe with a high relaxivity and a highly expressed molecular target is important. Additionally, the molecular probe must have a biokinetic profile for fast excretion of the probe, so imaging can be performed shortly after administration. The unbound probe should have a substantially lower relaxivity compared with the bound probe to minimize signal from unspecific binding. The fibrin-specific molecular probe used in this study was developed to fulfill these properties. The molecular probe is composed of a small peptide with fast-binding kinetics. It is linked to four gadolinium chelates to maximize the relaxivity, if the probe is bound to its target. A high longitudinal relaxivity for the bound probe of 64.3 ± 2.8 mmol/L^{-1}·per second^{-1} was reported at 3 T.[24] Because of the high relaxivity of the probe, a relatively low dose (10 μmol/kg^{-1}) was administered. The used dose was comparable to the applied dose in large animal models and the successful clinical feasibility trial.[18,36–38] The probability of gadolinium-induced toxicity is therefore reduced as such a low dose is used. This is especially relevant in the light of recent findings regarding nephrogenic systemic fibrosis.[39]

For the in vivo characterization of fibrin in aortic aneurysms, it is an important safety consideration that the administered probe does not interfere with the clotting cascade or other targets for therapeutic intervention. The fibrin-specific probe used in this study was designed to selectively bind fibrin and not its precursor, fibrinogen.[40,41] Different fibrin-targeted nanoparticles have also been applied for the experimental in vivo visualization of thrombi by other groups.[42,43] The probe used in our study is the only one that has already been successfully tested in a clinical setting.[18]

Limitations

The main difference between the experimental model used in this study, compared with human AAAs, is the different anatomic locations where the aneurysm develops. In patients,

AAAs develop in most cases in the infrarenal part of the aorta. In the ApoE$^{-/-}$ mouse model used in this study, AAAs develop in the suprarenal part of the aorta.[9,16,44] The exact mechanism responsible for this difference has not been elucidated yet. It has been hypothesized that the difference in blood pressure/hemodynamics and regional differences in the composition of the aortic wall might be responsible for this difference.[45] Compared with the different experimental animal models of AAAs, the ApoE$^{-/-}$ mouse model used in this study has the advantage that no surgical intervention is needed. AAAs develop spontaneously as a result of the continuous angiotensin II infusion with the associated increase blood pressure.

Conclusion

This study demonstrates that fibrin-specific molecular MR imaging enables the in vivo characterization of AAAs. The early formation of a focal mural hematoma, associated with the aortic dissection, could be detected before the dilation of the aorta. Additionally, changes in the fibrin composition of AAA-associated thrombi could be quantified and enable a differentiation between early fibrin-rich and advanced remodeled stable thrombi. Fibrin MRI could therefore provide a novel in vivo biomarker to improve the risk stratification of patients with aortic aneurysms.

Sources of Funding

The magnetic resonance imaging scanner is partly supported by Philips Healthcare. The study was funded by the British Heart Foundation (PG/09/061) and the DFG (MA 5943/3-1 and MA 5943/4-1).

Disclosures

None.

References

1. Gillum RF. Epidemiology of aortic aneurysm in the United States. *J Clin Epidemiol*. 1995;48:1289–1298.
2. Kniemeyer HW, Kessler T, Reber PU, Ris HB, Hakki H, Widmer MK. Treatment of ruptured abdominal aortic aneurysm, a permanent challenge or a waste of resources? Prediction of outcome using a multi-organ-dysfunction score. *Eur J Vasc Endovasc Surg*. 2000;19:190–196.
3. Bengtsson H, Sonesson B, Bergqvist D. Incidence and prevalence of abdominal aortic aneurysms, estimated by necropsy studies and population screening by ultrasound. *Ann N Y Acad Sci*. 1996;800:1–24.
4. Hallett JW Jr. Management of abdominal aortic aneurysms. *Mayo Clin Proc*. 2000;75:395–399.
5. Johnston KW, Rutherford RB, Tilson MD, Shah DM, Hollier L, Stanley JC. Suggested standards for reporting on arterial aneurysms. Subcommittee on reporting standards for arterial aneurysms, ad hoc committee on reporting standards, Society for Vascular Surgery and North American Chapter, International Society for Cardiovascular Surgery. *J Vasc Surg*. 1991;13:452–458.
6. Sakalihasan N, Limet R, Defawe OD. Abdominal aortic aneurysm. *Lancet*. 2005;365:1577–1589.
7. Farand P, Garon A, Plante GE. Structure of large arteries: orientation of elastin in rabbit aortic internal elastic lamina and in the elastic lamellae of aortic media. *Microvasc Res*. 2007;73:95–99.
8. Hellenthal FA, Buurman WA, Wodzig WK, Schurink GW. Biomarkers of AAA progression. Part 1: extracellular matrix degeneration. *Nat Rev Cardiol*. 2009;6:464–474.
9. Saraff K, Babamusta F, Cassis LA, Daugherty A. Aortic dissection precedes formation of aneurysms and atherosclerosis in angiotensin II-infused, apolipoprotein E-deficient mice. *Arterioscler Thromb Vasc Biol*. 2003;23:1621–1626.
10. Krettek A, Sukhova GK, Libby P. Elastogenesis in human arterial disease: a role for macrophages in disordered elastin synthesis. *Arterioscler Thromb Vasc Biol*. 2003;23:582–587.
11. Huffman MD, Curci JA, Moore G, Kerns DB, Starcher BC, Thompson RW. Functional importance of connective tissue repair during the development of experimental abdominal aortic aneurysms. *Surgery*. 2000;128:429–438.
12. Golledge J, Muller R, Clancy P, McCann M, Norman PE. Evaluation of the diagnostic and prognostic value of plasma D-dimer for abdominal aortic aneurysm. *Eur Heart J*. 2011;32:354–364.
13. Sidloff DA, Stather PW, Choke E, Bown MJ, Sayers RD. A systematic review and meta-analysis of the association between markers of hemostasis and abdominal aortic aneurysm presence and size. *J Vasc Surg*. 2014;59:528–535.e524.
14. Houard X, Rouzet F, Touat Z, Philippe M, Dominguez M, Fontaine V, Sarda-Mantel L, Meulemans A, Le Guludec D, Meilhac O, Michel JB. Topology of the fibrinolytic system within the mural thrombus of human abdominal aortic aneurysms. *J Pathol*. 2007;212:20–28.
15. Lederle FA, Wilson SE, Johnson GR, Reinke DB, Littooy FN, Acher CW, Ballard DJ, Messina LM, Gordon IL, Chute EP, Krupski WC, Busuttil SJ, Barone GW, Sparks S, Graham LM, Rapp JH, Makaroun MS, Moneta GL, Cambria RA, Makhoul RG, Eton D, Ansel HJ, Freischlag JA, Bandyk D. Immediate repair compared with surveillance of small abdominal aortic aneurysms. *N Engl J Med*. 2002;346:1437–1444.
16. Daugherty A, Manning MW, Cassis LA. Angiotensin II promotes atherosclerotic lesions and aneurysms in apolipoprotein E-deficient mice. *J Clin Invest*. 2000;105:1605–1612.
17. Overoye-Chan K, Koerner S, Looby RJ, Kolodziej AF, Zech SG, Deng Q, Chasse JM, McMurry TJ, Caravan P. EP-2104R: a fibrin-specific gadolinium-based MRI contrast agent for detection of thrombus. *J Am Chem Soc*. 2008;130:6025–6039.
18. Spuentrup E, Botnar RM, Wiethoff AJ, Ibrahim T, Kelle S, Katoh M, Ozgun M, Nagel E, Vymazal J, Graham PB, Gunther RW, Maintz D. MR imaging of thrombi using EP-2104R, a fibrin-specific contrast agent: initial results in patients. *Eur Radiol*. 2008;18:1995–2005.
19. Spuentrup E, Fausten B, Kinzel S, Wiethoff AJ, Botnar RM, Graham PB, Haller S, Katoh M, Parsons EC Jr, Manning WJ, Busch T, Gunther RW, Buecker A. Molecular magnetic resonance imaging of atrial clots in a swine model. *Circulation*. 2005;112:396–399.
20. Andia ME, Saha P, Jenkins J, Modarai B, Wiethoff AJ, Phinikaridou A, Grover SP, Patel AS, Schaeffter T, Smith A, Botnar RM. Fibrin-targeted magnetic resonance imaging allows in vivo quantification of thrombus fibrin content and identifies thrombi amenable for thrombolysis. *Arterioscler Thromb Vasc Biol*. 2014;34:1193–1198.
21. Henke J, Baumgartner C, Roltgen I, Eberspacher E, Erhardt W. Anaesthesia with midazolam/medetomidine/fentanyl in chinchillas (*Chinchilla lanigera*) compared to anaesthesia with xylazine/ketamine and medetomidine/ketamine. *J Vet Med A Physiol Pathol Clin Med*. 2004;51:259–264.
22. Botnar RM, Wiethoff AJ, Ebersberger U, Lacerda S, Blume U, Warley A, Jansen CH, Onthank DC, Cesati RR, Razavi R, Marber MS, Hamm B, Schaeffter T, Robinson SP, Makowski MR. In vivo assessment of aortic aneurysm wall integrity using elastin-specific molecular magnetic resonance imaging. *Circ Cardiovasc Imaging*. 2014;7:679–689.
23. Makowski MR, Wiethoff AJ, Blume U, Cuello F, Warley A, Jansen CH, Nagel E, Razavi R, Onthank DC, Cesati RR, Marber MS, Schaeffter T, Smith A, Robinson SP, Botnar RM. Assessment of atherosclerotic plaque burden with an elastin-specific magnetic resonance contrast agent. *Nat Med*. 2011;17:383–388.
24. Makowski MR, Forbes SC, Blume U, Warley A, Jansen CH, Schuster A, Wiethoff AJ, Botnar RM. In vivo assessment of intraplaque and endothelial fibrin in ApoE (−/−) mice by molecular MRI. *Atherosclerosis*. 2012;222:43–49.
25. King VL, Lin AY, Kristo F, Anderson TJ, Ahluwalia N, Hardy GJ, Owens AP III, Howatt DA, Shen D, Tager AM, Luster AD, Daugherty A, Gerszten RE. Interferon-gamma and the interferon-inducible chemokine CXCL10 protect against aneurysm formation and rupture. *Circulation*. 2009;119:426–435.

26. Anidjar S, Dobrin PB, Eichorst M, Graham GP, Chejfec G. Correlation of inflammatory infiltrate with the enlargement of experimental aortic aneurysms. *J Vasc Surg*. 1992;16:139–147.
27. Koch AE, Haines GK, Rizzo RJ, Radosevich JA, Pope RM, Robinson PG, Pearce WH. Human abdominal aortic aneurysms. Immunophenotypic analysis suggesting an immune-mediated response. *Am J Pathol*. 1990;137:1199–1213.
28. Luk A, Leong S, Soor G, Borger M, Butany J. Histological analysis of aortic dissections following previous cardiovascular surgery. *Cardiovasc Pathol*. 2008;17:199–205.
29. Segreto A, Chiusaroli A, De Salvatore S, Bizzarri F. Biomarkers for the diagnosis of aortic dissection. *J Card Surg*. 2014;29:507–511.
30. Matsumura JS, Pearce WH, McCarthy WJ, Yao JS. Reduction in aortic aneurysm size: early results after endovascular graft placement. EVT Investigators. *J Vasc Surg*. 1997;25:113–123.
31. Lanza GM, Cui G, Schmieder AH, Zhang H, Allen JS, Scott MJ, Williams T, Yang X. An unmet clinical need: the history of thrombus imaging. *J Nucl Cardiol*. 2017. Available at: https://link.springer.com/article/10.1007%2Fs12350-017-0942-8. Accessed April 1, 2018.
32. Blasi F, Oliveira BL, Rietz TA, Rotile NJ, Day H, Naha PC, Cormode DP, Izquierdo-Garcia D, Catana C, Caravan P. Radiation dosimetry of the fibrin-binding probe (6)(4)Cu-FBP8 and its feasibility for PET imaging of deep vein thrombosis and pulmonary embolism in rats. *J Nucl Med*. 2015;56:1088–1093.
33. Blasi F, Oliveira BL, Rietz TA, Rotile NJ, Naha PC, Cormode DP, Izquierdo-Garcia D, Catana C, Caravan P. Multisite thrombus imaging and fibrin content estimation with a single whole-body PET scan in rats. *Arterioscler Thromb Vasc Biol*. 2015;35:2114–2121.
34. Quill DS, Colgan MP, Sumner DS. Ultrasonic screening for the detection of abdominal aortic aneurysms. *Surg Clin North Am*. 1989;69:713–720.
35. Yuan C, Kerwin WS, Ferguson MS, Polissar N, Zhang S, Cai J, Hatsukami TS. Contrast-enhanced high resolution MRI for atherosclerotic carotid artery tissue characterization. *J Magn Reson Imaging*. 2002;15:62–67.
36. Botnar RM, Buecker A, Wiethoff AJ, Parsons EC, Katoh M, Katsimaglis G, Weisskoff RM, Lauffer RB, Graham PB, Gunther RW, Manning WJ, Spuentrup E. In vivo magnetic resonance imaging of coronary thrombosis using a fibrin-binding molecular magnetic resonance contrast agent. *Circulation*. 2004;110:1463–1466.
37. Spuentrup E, Katoh M, Buecker A, Fausten B, Wiethoff AJ, Wildberger JE, Haage P, Parsons EC, Botnar RM, Graham PB, Vettelschoss M, Gunther RW. Molecular MR imaging of human thrombi in a swine model of pulmonary embolism using a fibrin-specific contrast agent. *Invest Radiol*. 2007;42:586–595.
38. Bellin M-F. MR contrast agents, the old and the new. *Eur J Radiol*. 2006;60:314–323.
39. Heverhagen JT, Krombach GA, Gizewski E. Application of extracellular gadolinium-based MRI contrast agents and the risk of nephrogenic systemic fibrosis. *Rofo*. 2014;186:661–669.
40. Jaffer FA, Libby P, Weissleder R. Molecular imaging of cardiovascular disease. *Circulation*. 2007;116:1052–1061.
41. Sirol M, Fuster V, Badimon JJ, Fallon JT, Moreno PR, Toussaint J-F, Fayad ZA. Chronic thrombus detection with in vivo magnetic resonance imaging and a fibrin-targeted contrast agent. *Circulation*. 2005;112:1594–1600.
42. Flacke S, Fischer S, Scott MJ, Fuhrhop RJ, Allen JS, McLean M, Winter P, Sicard GA, Gaffney PJ, Wickline SA, Lanza GM. Novel MRI contrast agent for molecular imaging of fibrin: implications for detecting vulnerable plaques. *Circulation*. 2001;104:1280–1285.
43. Winter PM, Caruthers SD, Yu X, Song S-K, Chen J, Miller B, Bulte JWM, Robertson JD, Gaffney PJ, Wickline SA, Lanza GM. Improved molecular imaging contrast agent for detection of human thrombus. *Magn Reson Med*. 2003;50:411–416.
44. Wang YX, Martin-McNulty B, Freay AD, Sukovich DA, Halks-Miller M, Li WW, Vergona R, Sullivan ME, Morser J, Dole WP, Deng GG. Angiotensin II increases urokinase-type plasminogen activator expression and induces aneurysm in the abdominal aorta of apolipoprotein E-deficient mice. *Am J Pathol*. 2001;159:1455–1464.
45. Halloran BG, Davis VA, McManus BM, Lynch TG, Baxter BT. Localization of aortic disease is associated with intrinsic differences in aortic structure. *J Surg Res*. 1995;59:17–22.

SUPPLEMENTAL MATERIAL

Data S1

Supplementary Methods

In vivo molecular MR imaging

Following the 3D IR fast gradient echo scans, a quantitative T1 mapping sequence (3D) was acquired. Part of the sequence are two inversion-recovery prepared modified Look-Locker 'trains'.[1, 2] Each trains is initiated by a non-selective IR pulse (inversion pulse) that is defined by a specific initial IR time (inversion time, 12, 73ms). The IR pulse is followed by eight segmented readouts for the reconstructed eight individual images. The inversion times are defined as the time from the center of the preparation pulse to the acquisition of the k0 profile in k space. A delay of 500ms is inserted in-between each image acquisition to minimize potential saturation effects and to enable an accurate quantification of long T1 times. Imaging parameters of the T1 mapping sequences were:

Matrix = 180 x 151, field of view = 18 x 36 mm, voxel size 0.2 x 0.2 x 0.5 mm, repetition time (TR) = 9.8 ms, echo time (TE) = 5.1 ms, acquisition window = 157 ms, flip angle = 8°. A set of 16 source images resulted from the two imaging trains. T1 values were calculated pixel by pixel using a three-parameter curve fitting technique of the longitudinal magnetization Mz(TI), which included a T1 correction:[3]

$$M_Z(TI)=M_0^*- (M_0+M_0^*)^{e-(TI((1/T1)-(1/TR)\ln(\cos \alpha)))}$$

T1 then can be calculated as:[4]

$$T1=T1^* (((M_0+M_0^*)/(M_0^*)) – 1)$$

M0 represents the equilibrium magnetization. The longitudinal magnetization is sampled during

its recovery. Therefore, the relaxation process is influenced by the constant application of RF-pulses which results in the assessment of an apparent relaxation time T1* (T1*<T1; R1=1/T1; $1/T1^* = T/T1 + 1/T1_{LookLocker}$) and a reduction in the equilibrium magnetization M0*.

Following the completion of MR scanning, mice were euthanized by dislocation of the neck. Tissues were then harvested for further processing. These techniques have been previously described in [5, 6].

Aortic aneurysm morphometry

The suprarenal aorta was excised including the last pair of intercostal artery and the right renal artery. Landmarks for co–registration were the left renal artery and the last pair of intercostal artery. A time–of–flight (TOF) angiogram was always acquired before planning of the DE–MRI (delayed enhancement magnetic resonance imaging) imaging slices. Based on the 3D maximum intensity projection (MIP) reconstructed from the TOF angiograms, high–resolution DE–MRI imaging slices could be planned exactly perpendicular to the course of the aorta. All morphometric analyses were made on elastin–stained sections. Morphometry was performed using ImageProPlus software (ImageProPlus, MediaCybernetics). The areas enclosed by the adventitia and the lumen were recorded. %EvG stain per adventitial area was assessed using ImageProPlus. Segmentation of elastic fibers was based on the color profile of the elastic fibers in the media of the vessel wall on the EvG stained section. These techniques have been previously described in [5].

Competition experiments:

In vivo competition experiments (supplementary figure 2) were performed in ApoE-/- mice

following the four-week infusion of angiotensin-II (Ang-II, 1 microgram kg-1 min). During imaging session one initially a precontrast scan, prior to the administration of the fibrin specific probe, was performed. Following the precontrast scan, the fibrin specific molecular MR probe (EP2104R, 10 µmol kg–1) was administered and imaging was performed using a T1 delayed enhancement MRI sequence. 48 hours later, imaging session two was performed. Initially a precontrast scan was acquired to confirm that no residual binding is present. In the next step, 100 µmol kg-1 of the unlabeled imaging probe peptide were administered. Subsequently, another T1 delayed enhancement MRI was performed to exclude an increase in signal enhancement. Following this scan, the Gd-labeled fibrin specific molecular MR probe (EP2104R, 10 µmol kg–1) was administered and another T1 delayed enhancement MRI was performed.

Figure S1. Organization of study with time-course of in vivo imaging and ex vivo tissue analysis.

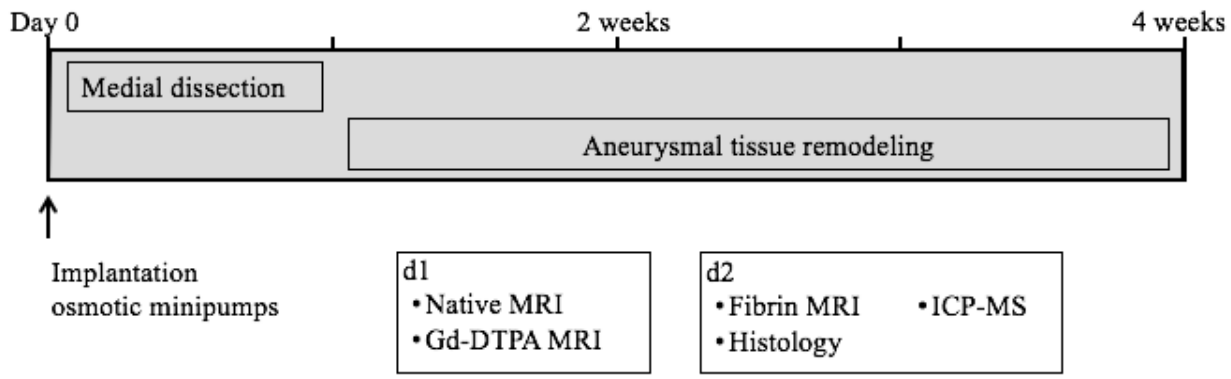

Setup and time-course of the animal experiments indicating the different timepoints at which in vivo MR imaging and ex vivo tissue analysis was performed. It was demonstrated by different previous studies that media dissection is the initial event in AAA formation in the animal model used[7]. In advanced stages of AAA development, the fibrin rich thrombus gets increasingly remodeled and stabilized with extracellular matrix proteins including collagen and elastin.

Figure S2. In vivo competition experiments in ApoE-/- mice with aortic aneurysms.

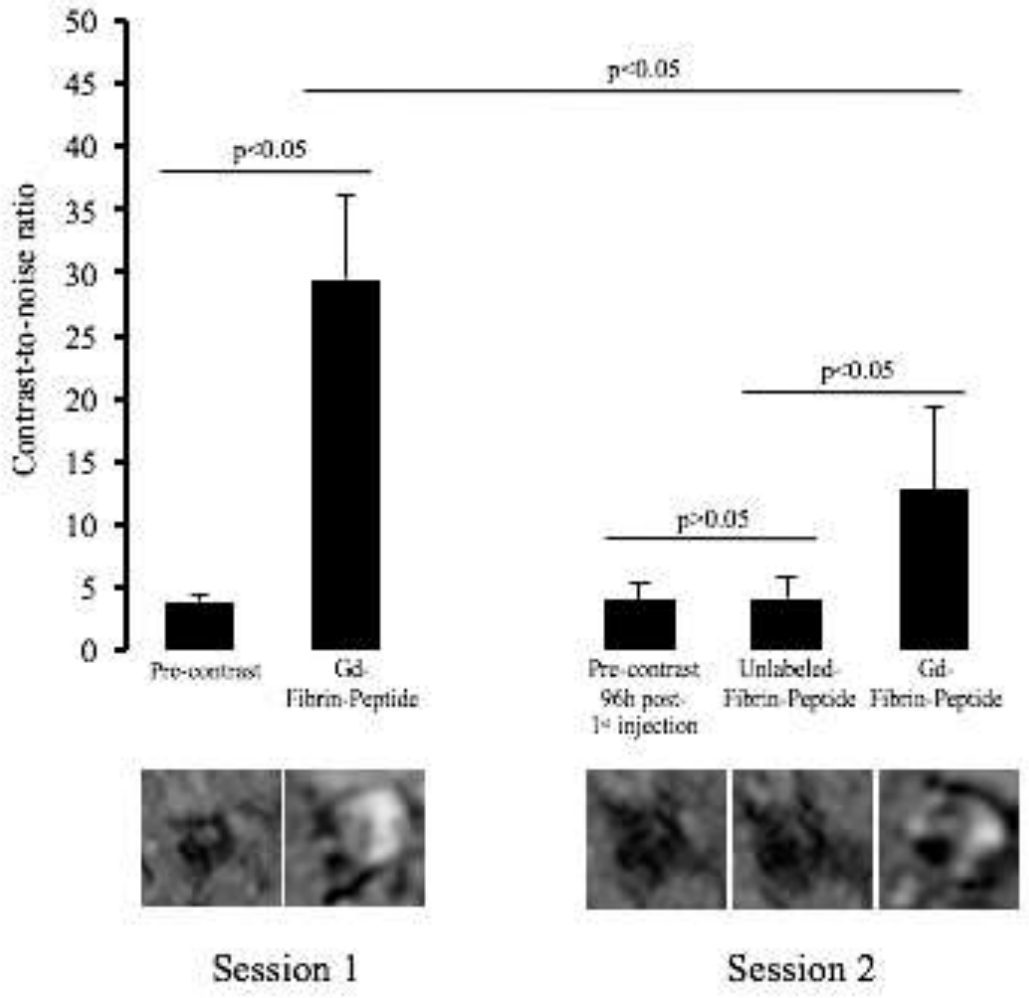

The signal enhancement of precontrast scans in imaging session one did not differ from the signal enhancement of the other investigated animals at the same time point in this study (4 weeks of angiotensin II infusion). The administration of the gadolinium labeled fibrin specific molecular MR probe resulted in a marked increase of, compared to the precontrast scan. 48 hours later at imaging session two, initially a precontrast scan was performed. The precontrast scan yielded a CNR which was not significantly different from the precontrast scan during imaging session one. In the next step, the injection of the unlabeled imaging probe peptide did not result in a significant increase of CNR. In the final step, the Gd-labeled fibrin specific molecular MR probe (EP2104R) was administered. This resulted in a significantly decreased CNR compared to the probe injection during session one. No significant difference was found between the precontrast scan during session one and session two.

Supplemental References:

1. Look DC, Locker DR. Time saving in measurement of NMR and EPR relaxation times. *Rev Sci Instrum*. 1970;41:250-251.

2. Messroghli DR, Radjenovic A, Kozerke S, Higgins DM, Sivananthan MU, Ridgway JP. Modified Look-Locker inversion recovery (MOLLI) for high-resolution T1 mapping of the heart. *Magnetic Resonance in Medicine*. 2004;52:141-146.

3. Karlsson M, Nordell B. Phantom and in vivo study of the Look-Locher T1 mapping method. *Magn Reson Imaging*. 1999;17:1481-8.

4. Deichmann R, Hahn D, Haase A. Fast T1 mapping on a whole-body scanner. *Magnetic Resonance in Medicine*. 1999;42:206-209.

5. Botnar RM, Wiethoff AJ, Ebersberger U, Lacerda S, Blume U, Warley A, Jansen CH, Onthank DC, Cesati RR, Razavi R, Marber MS, Hamm B, Schaeffter T, Robinson SP, Makowski MR. In vivo assessment of aortic aneurysm wall integrity using elastin-specific molecular magnetic resonance imaging. *Circ Cardiovasc Imaging*. 2014;7:679-89.

6. Makowski MR, Wiethoff AJ, Blume U, Cuello F, Warley A, Jansen CH, Nagel E, Razavi R, Onthank DC, Cesati RR, Marber MS, Schaeffter T, Smith A, Robinson SP, Botnar RM. Assessment of atherosclerotic plaque burden with an elastin-specific magnetic resonance contrast agent. *Nat Med*. 2011;17:383-8.

7. Saraff K, Babamusta F, Cassis LA, Daugherty A. Aortic dissection precedes formation of aneurysms and atherosclerosis in angiotensin ii-infused, apolipoprotein e-deficient mice. *Arterioscler Thromb Vasc Biol*. 2003;23:1621-1626.